Heliyon 10 (2024) e31168

Contents lists available at ScienceDirect

Heliyon

journal homepage: www.cell.com/heliyon

Research article

Testing the inhibition efficiency of the castor oil leaf as corrosion inhibitor of mild steel in H_2SO_4

M. Omotioma [a], O.D. Onukwuli [b], I.A. Nnanwube [c,*]

[a] Department of Chemical Engineering, Enugu State University of Science and Technology, P.M.B. 01660, Enugu, Nigeria
[b] Department of Chemical Engineering, Nnamdi Azikiwe University, P.M.B. 5025, Awka, Anambra State, Nigeria
[c] Department of Chemical Engineering, Madonna University, Akpugo Campus, 402105, Akpugo, Enugu State, Nigeria

ARTICLE INFO

Keywords:
Frumkin isotherm
Corrosion inhibitor
Methyl nicotinate
Pyridine-4-carbohydrazide
ANN

ABSTRACT

This study focused on the testing of castor oil leaf as corrosion inhibitor of mild steel in H_2SO_4. It involved the examination of the dynamics of molecular forces at the inhibitor and mild steel interface. Findings of the study will promote industrial diversification of castor oil leaf. On the experiment, bio-molecular compounds of the leaf were identified by gas chromatography mass spectrophotometer. Then, gravimetric and potentiodynamic polarization techniques were employed, where the efficacy and type of the inhibitor were determined. Considering the gravimetric process, factors of inhibitor concentration (0.2 g/L - 1.0 g/L), temperature (303 K–333 K) and time (8 h–24 h) were considered, with the inhibitor efficiency as the response. The efficiency was determined and optimized using response surface methodology (RSM) and artificial neural network (ANN). On the other hand, potentiodynamic polarization process was used to identify the type of inhibitor. Adsorption quantities were ascertained through the subjection of the experimental raw data to various adsorption isotherms. The analyses showed that castor oil leaf contains methyl nicotinate and pyridine-4-carbohydrazide. The bio-molecular compounds possess heteroatoms (N, S and O), signifying strong corrosion inhibitive tendencies. High efficiency (96.25 %) was obtained, with ANN having better prediction capability than the RSM. Potentiodynamic polarization curves revealed castor oil leaf as mixed-type inhibitor. On the adsorption phenomenon, the process of the inhibition was best fitted by Frumkin isotherm, revealing physical adsorption mechanism of Gibb's free energy less than −40 kJ/mol. As a mixed-type inhibitor, castor oil leaf should be applied for mitigation of anodic and cathodic corrosion.

1. Introduction

Modern engineering has a wide range of constructions involving usage of various kinds of steel. As such, researchers oftentimes study steel in various media with the intention of providing information that influences steel selection for engineering application [1–4]. In construction/operational works, there are no general rules on steel selection, but logical decision on the choice of steel embroils a consideration of relevant characteristics. Such characteristics include availability, ease of fabrication, physico-chemical properties and relative cost. Sometimes, decisions on choice of steel or other metals are based on economic factors rather than due consideration of the physico-chemical parameters. Mechanical and physical properties of metals may be expressed as constant, but

* Corresponding author.
E-mail address: ik.nnanwube@gmail.com (I.A. Nnanwube).

https://doi.org/10.1016/j.heliyon.2024.e31168
Received 31 August 2023; Received in revised form 25 April 2024; Accepted 11 May 2024
Available online 13 May 2024

their chemical characteristics depend on the operational environment (see Fig. 10).

As a metal, mild steel (rich in iron) is chemically unstable because it depends on the prevailing environment. It undergoes chemical and/or electrochemical reaction with its environment to attain stability. In general, chemical reactivity of metal is connected to its natural propensity of oxidation, as it has tendency to return to its natural state by chemical reactions with the constituents of the environment [5,6]. Such oxidative or chemical destruction of metal is regarded as corrosion. So, corrosion of metal is a natural process, where the rate of oxidation of metal is a function of the change in standard Gibb's free energy (ΔGo). Higher negative values of ΔGo show higher impulsiveness of reaction and thus higher rate of corrosion. As metals are exposed to corrosive environment (acid or alkaline solution) in numerous industrial operations, they deteriorate/corrode [7,8].

Corrosion is an oxidative or chemical obliteration of materials (typically metals and alloys) as a result of the contact of the materials with their environment [9–11]. It is a huge issue for scientists and engineers. Over the years, copious failures of industrial facilities due to corrosion are common in; aerospace and defense, automotive, nuclear, electrical and electronics, marine and off-shore, and chemical industries. Corrosion can cause higher costs for engineering and transportation systems. For instance, narrowed pipe diameters resulting from corrosion deposits decrease pumping capability. Also, high replacement frequency of vessels, pipes, heaters, radiators, valves, and meters are observed because of corrosion damage. Severe consequences of corrosion process have become a problem of worldwide significance. As such, researchers and industrialists take issue of structural maintenance (that can prevent corrosion) very seriously.

The maintenance of metal-based structures requires operations such as pickling (acid cleaning), in which metal (such as mild steel) surface is cleaned by acid medium [12,13]. Such metal-acid contact (occasioned by acid cleaning) often creates a condition for the metal dilapidation as side effect of the pickling. As such, there is need to control corrosion using acid cleaning solution (1 M H_2SO_4) with additive (inhibitor). Hence, corrosion scientists and engineers have increased research interest in developing corrosion inhibitors. Inhibitor forms protective covering over the surface of the metal, thereby isolating it from the environment, and subsequently preventing degradation process [13, 14, 15, 16, 17]. Synthetic chemical inhibitor is viable for corrosion control, but its application is discouraged due to environmental concerns. Qurishi et al. [18] reported that bio-inspired hetero-cyclic organic molecules have high import as possible alternatives to the present inhibitor chemistries. Thus, research efforts are now geared towards development of eco-friendly inhibitors [10,18–20]. In this study, castor oil leaf was chosen as inhibitor in order to sufficiently explore and diversify its industrial applications.

2. Materials and method

2.1. Materials and equipment

Materials and reagents deployed in this study include mild steel, castor oil leaf, distilled water, ethanol, and H_2SO_4. Equipment/devices used in the study include; water bath with thermostat, gas chromatography-mass spectrometer. Chemicals used in this study are of analytical grade.

2.2. Determination of chemical constituents of castor oil leaf extract

Chemical constituent of the castor oil leaf extract was identified by gas chromatography-mass spectrometer (GCMS-QP2010 PLUS; SHIMADZU). The procedure used is similar to that of Onukwuli and Omotioma [21]. Features of gas chromatography (GC) and mass spectrometry (MS) were jointly applied to categorize different chemical constituents within the castor oil extract. The extract was separated into individual molecular constituents in the GC. They were accelerated along the column with nitrogen as an inert gas. Then, separate constituents emerged from the column and flew to the MS, where they were appropriately identified.

2.3. Gravimetric study

Gravimetric technique used by previous authors was adopted [22–26]. Major materials and reagent employed include mild steel, H_2SO_4 and castor oil leaf. They were prepared/processed and used for the experimental study. The mild steel has the following composition; Mn, 0.11 %; C, 0.23 %; Cr, 0.01 %; Si, 0.02 %; P, 0.02 %; S, 0.02 %; Cu, 0.01 %; Ni, 0.02; and Fe, 99.56 %). For the concentration of the acid, 1 M H_2SO_4 was used; prepared by adding 54.35 ml H_2SO_4 (specific gravity of 1.84; 98 % pure) into 945.65 ml distilled water in a cylinder (1000 ml). In a batch process, plant extract was obtained by soaking 30.0 g of the ground castor oil leaf (0.85 mm particle size) in 1000 ml of ethanol (99.7 % v/v) for a time-period of two days. This was followed by filtration and subsequent separation of the extract from the ethanol. 10 g of the extract was dissolved in 1000 ml of the prepared H_2SO_4. The stock solution of 10 g/L was used to obtain various concentrations of the extract (0.2 g/L - 1.0 g/L) through a dilution process.

For the corrosion inhibition experiment, weighed mild steel was put into 250 ml open beaker containing 200 ml of 1 M H_2SO_4 (blank). Also, mild steel samples were put into 250 ml open beakers containing 200 ml of 1 M H_2SO_4 with various concentrations of the extract. With the aid of Design Expert Software (version 11), the central composite design tool of RSM was used to design the experiment in line with the procedure used by previous researchers (12, 24). Inhibitor concentration (0.2 g/L - 1.0 g/L), temperature (303 K–333 K) and time (8 h–24 h) were the factors considered while efficiency of the inhibitor (calculated using Equation (1)) was the response of the study. The RSM aided the analysis of the response in line with previous reports [12,27]. The Analysis of Variance and graphical representation of the inhibition process were presented. Coded factor based mathematical model was established, and optimum parameters obtained. The corrosion rate (CR) is given as Equation (2).

$$IE\% = \frac{\omega_0 - \omega_1}{\omega_0} * 100 \tag{1}$$

$$CR = \frac{w_i - w_f}{At} \tag{2}$$

where ω_1 and ω_0 denote the weight loss values in presence and absence of inhibitor, respectively, w_i and w_f denote the initial and final weights of the metal, t and *A* symbolize time of immersion and area of the mild steel coupon respectively.

Levenberg-Marquardt trained standard two-layer feed-forward neural network was deployed in the ANN analysis of the optimization process [28,29]. Network created from the data was trained and evaluated to ascertain its performance using mean square error and regression analysis. Then, iterative process of improving the performance was adopted. In the ANN modeling process, three kinds of the network samples were considered; training, validation and testing.

2.4. Comparative analysis of RSM and ANN results

Comparative analysis of the results was achieved by applying techniques used by previous authors [29,30]. Equations (3)–(5) respectively were employed in the determination of the statistical criteria; coefficient of determination (R^2), root mean square error (RMSE), and the standard error of prediction (SEP):

$$R^2 = 1 - \frac{\sum_{i=1}^{n}\left(Y_{exp,i} - Y_{pred.,i}\right)^2}{\sum_{i=1}^{n}\left(Y_{exp,i} - Y_{pred.,ave}\right)^2} \tag{3}$$

$$RMSE = \left(\frac{1}{n}\sum_{i-1}^{n}\left(Y_{pred} - Y_{exp}\right)^2\right)^{1/2} \tag{4}$$

$$SEP = \frac{RMSE}{Y_{exp.\ ave}} * 100 \tag{5}$$

where n is the number of sample points, Y_{pred} is the predicted inhibition efficiency, Y_{exp} is the experimentally determined value of the Inhibition efficiency, $Y_{exp.\ ave}$ is experimental average, Y_{exp} is experimental value.

2.5. Potentiodynamic polarization (PDP) study

PDP was used to identify the types of inhibitors that castor oil leaf has. Potentiodynamic polarization study was carried out according to the method used by previous research reports [12,27,31]. It was conducted with the aid of potentiostat/galvanostat 263 electrochemical workstation. It involved the application of conventional three-eletrode corrosion cell, where saturated calomel electrode (SCE) and graphite rod were respectively used as reference and counter electrodes. Sample of the mild steel (which served as working electrode) was fixed in epoxy resin with a surface area of 1 cm^2 exposed to the H_2SO_4 media. Electrochemical measurements (at the end of 30 min of immersion) were done in aerated and unstirred media, which allowed the open circuit potential (OCP) to attain steady state. The temperature was fixed at 30 ± 1 °C, and the polarization study was performed in the range of ±250 mV versus corrosion potential at a scan rate of 0.333 mV/s.

2.6. Analysis of the adsorption isotherms

The data of the degree of surface coverage (Equation (6); which has direct relationship with efficiency, Equation (1) at various inhibitor's concentrations aided the examination of the application of various adsorption isotherms; the suitability of Langmuir, Frumkin, Temkin and Flory-Huggins of Equations (7)–(10) respectively [12,26]). Then, the Gibb's energy (ΔG_{ads}) was obtained using Equation (11), that depends on gas constant (*R*), temperature (*T*) and adsorption equilibrium constant (*K*).

$$\theta = \frac{\omega_0 - \omega_1}{\omega_0} \tag{6}$$

$$log\frac{C}{\theta} = \log C - logK \tag{7}$$

$$\log\left((C) * \left(\frac{\theta}{1-\theta}\right)\right) = 2.303logK + 2\alpha\theta \tag{8}$$

$$\theta = -\frac{2.303logK}{2a} - \frac{2.303logC}{2a} \tag{9}$$

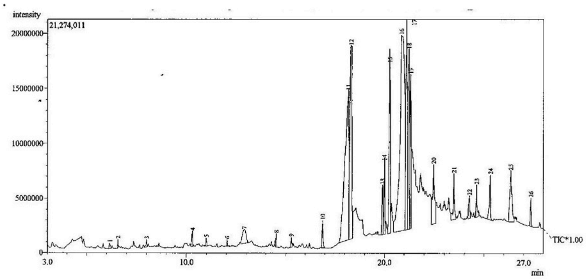

Fig. 1. The GC MS chromatogram of castor oil leaf.

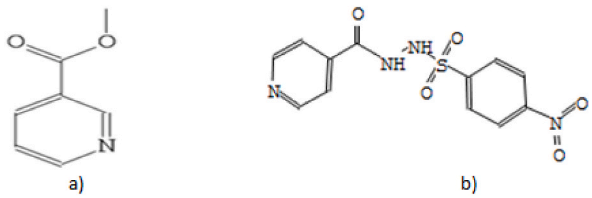

Fig. 2. Molecular structure a) Methyl nicotinate ($C_7H_7NO_2$), and b) Pyridine-4-carbohydrazide ($C_{12}H_{10}N_4O_5S$).

Table 1
The RSM result of the corrosion combined.

Std No.	Run No.	A: Inh. conc.(g/L)	B: T (K)	C: t (hr)	IE (%)
5	1.0	0.2	303.0	24	77.24
3	2.0	0.2	333.0	8	68.15
14	3.0	0.6	318.0	24	92.62
13	4.0	0.6	318.0	8	92.29
2	5.0	1.0	303.0	8	83.12
10	6.0	1.0	318.0	16	91.43
16	7.0	0.6	318.0	16	96.25
9	8.0	0.2	318.0	16	79.01
12	9.0	0.6	333.0	16	79.89
4	10.0	1.0	333.0	8	71.92
18	11.0	0.6	318.0	16	96.25
15	12.0	0.6	318.0	16	96.25
1	13.0	0.2	303.0	8	69.54
20	14.0	0.6	318.0	16	96.25
19	15.0	0.6	318.0	16	96.25
7	16.0	0.2	333.0	24	70.06
8	17.0	1.0	333.0	24	75.25
11	18.0	0.6	303.0	16	93.65
6	19.0	1.0	303.0	24	92.07
17	20.0	0.6	318.0	16	96.25

$$log\left(\frac{\theta}{C}\right) = log\,K + xlog(1-\theta) \quad (10)$$

$$\Delta G_{ads} = -2.303RTlog(55.5K) \quad (11)$$

α is the lateral interaction term, 'a' is the attractive parameter, C is the inhibitor's concentration, θ is the surface coverage, and x is the size parameter.

3. Results and discussion

3.1. Chemical constituents of the castor oil leaf

In Fig. 1, the chromatogram of the castor oil leaf shows various levels of peaks. The peaks represent various compounds as determined by gas chromatography mass spectrophotometer. The chromatogram revealed the presence of methyl nicotinate; methyl ester; pyridine-4-carbohydrazide; 4-ketopimelic; 4-oxoheptanedioic acid; succinic acid, ethyl hydrogen succinate. It also contains

Table 2
Model's fit summaries.

Model/parameter	Value of sequential probability	Adjusted R^2	Predicted R^2	
Linear-model	0.1842	0.1146	−0.3245	
2FI-model	0.9079	−0.0463	−4.1042	
Quadratic-model	<0.0001	0.9739	0.9047	Suggested
Cubic-model	0.0410	0.9899	−2.9100	Aliased

Table 3
ANOVA of the model.

$$\text{Inhibition efficiency} = +95.67 + 4.98A - 5.04B + 2.22C - 2.43AB - 1.43BC - 9.59A^2 - 8.03B^2 - 2.35C^2 \quad (12)$$

$$\text{Inhibition efficiency} = -3588.50065 + 211.52250\text{Inhibitor conc.} + 22.80989\text{Temp.} + 5.16973\text{Time} - 0.405208\text{Inh. conc.} * \text{Temp.} - 0.011885\text{Temp.} * \text{Time} - 59.90625\text{Inh. conc.}^2 - 0.035711\ \text{Temp.}^2 - 0.036719\text{Time}^2 \quad (13)$$

Parameter	Sum of Squares	Degree of freedom	Mean Square	Fisher test value	Probability value	Remark
Model	2135.56	9.0	237.28	79.70	<0.0001	Significant
A (Inh. conc.)	247.90	1.0	247.90	83.27	<0.0001	
B (Temp.)	253.51	1.0	253.51	85.16	<0.0001	
C (Time)	49.37	1.0	49.37	16.58	0.0022	
AB.	47.29	1.0	47.29	15.88	0.0026	
AC.	0.8911	1.0	0.8911	0.2993	0.5963	
BC.	16.27	1.0	16.27	5.47	0.0415	
Aˆ2	252.65	1.0	252.65	84.86	<0.0001	
Bˆ2	177.54	1.0	177.54	59.64	<0.0001	
Cˆ2	15.19	1.0	15.19	5.10	0.0475	
Residual	29.77	10.0	2.98			
Lack of Fit	29.77	5.0	5.95			
Pure Error	0.0000	5.0	0.0000			
Cor Total	2165.33	19.0				
Std. Dev.	1.73		R^2		0.9863	
Mean	85.69		Adj. R^2		0.9739	
C.V. %	2.01		Pred. R^2		0.9047	
			Adeq Pre.		22.9619	

benzene acetaldehyde, 3-pyridinecarboxylic acid; nicotinic acid, methyl 3-pyridinecarboxylate; methyl ester of pyridine-3-carboxylic acid); butanedioic acid, diethyl ester; 9-hexadecenoic acid); oxacycloheptadecan-2-one. The predominant bio-molecular structures are displayed in Fig. 2; a) methyl nicotinate ($C_7H_7NO_2$), and b) pyridine-4-carbohydrazide ($C_{12}H_{10}N_4O_5S$). Methyl nicotinate and pyridine-4-carbohydrazide of the castor oil leaf contain heteroatoms of O, N and S. Presence of the heteroatoms, antioxidants as well as lengthy hydrocarbon chain revealed that the material is highly suitable for corrosion control [6,16,18,21,24].

3.2. Results of the RSM

RSM results of the efficiency of castor oil leaf (inhibitor) are presented in Table 1. It shows the interactive impact of the variables of inhibitor concentration, temperature and time on the inhibitor's efficiency. Highest efficiency of 96.25 % was recorded at a concentration of 0.6 g/L, temperature of 318 K and time of 16 h. Recorded excellent efficiency may be attributed to heteroatoms and biomolecules with hydrocarbon chain [16,18]. Layer of the molecules of the castor oil leaf may have efficiently isolated the metal from the aggressive H_2SO_4 solution.

3.2.1. Model's fit summaries and the analysis of variance (ANOVA)

Model's fit summaries and the analysis of variance (ANOVA) are respectively presented in Tables 2 and 3. In Table 2, values of R^2 for the linear and 2FI are not close to one (1). The quadratic model is suggested as best fitted model because the predicted R^2 of 0.9047 is close to 1; also, it is very close to the adjusted R^2 of 0.9739. It shows that the quadratic model can effectively predict the empirical data. Cubic model is not suggested as the best fitted model because the predicted R^2 is not in reasonable agreement with the adjusted R^2. In Table 3, Degree of freedom (Df), value of Fisher test (F-test) and probability value (p-value) were revealed as 9, 79.70 and <0.0001 respectively. The model F-value of 79.70 means that the model is significant, because only 1 out of 100 prospects of an F-value as large as 79.70 could happen owed to noise. Probability value (p-value) less than 5 % indicate that the terms of the model are significant. In this circumstance Aˆ2, Bˆ2, Cˆ2, AB, BC, A, B, C are significant terms of the quadratic equation. Adequate precision of 22.962 indicates an acceptable signal. Thus, the generated model is useful for routing the design space. The models in terms of coded and actual factors are as expressed in Equations (12) and (13) respectively. The coded model is suitable for making predictions about

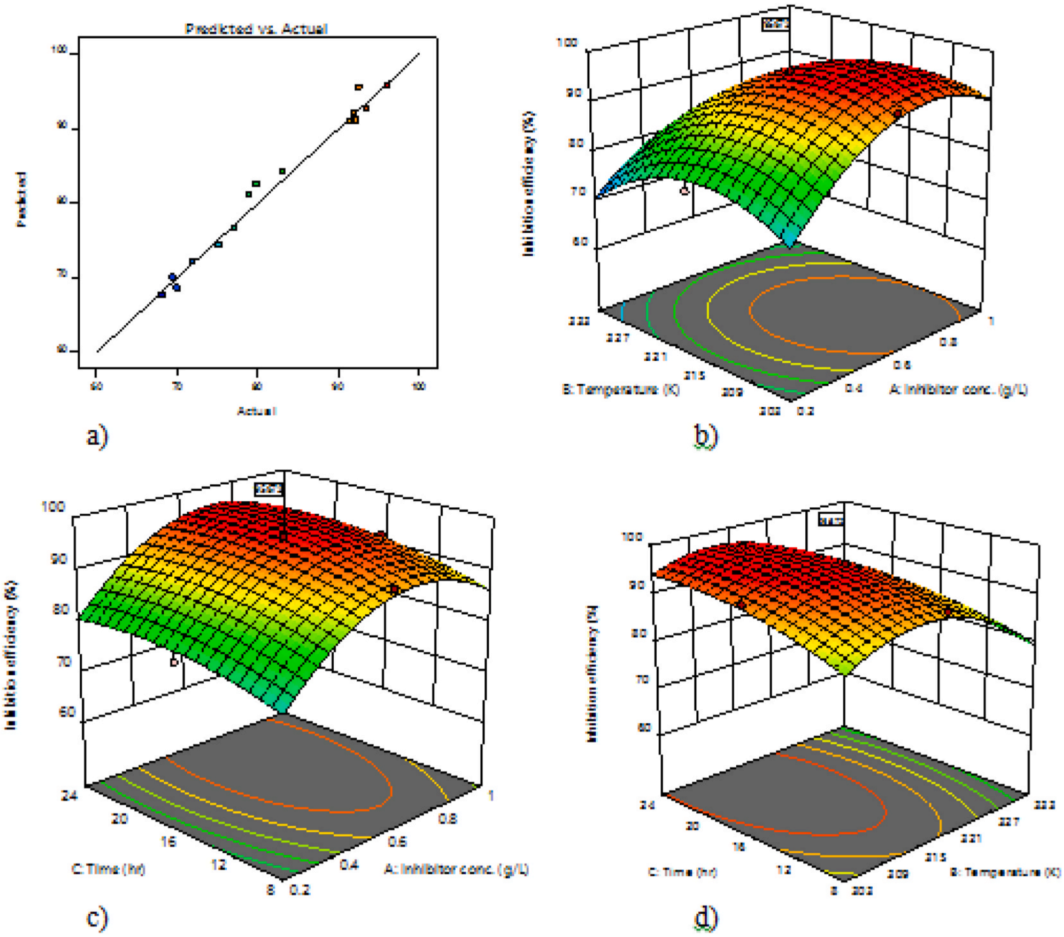

Fig. 3. Efficiency of castor oil leaf as function of the interactive effects of the factors: a) Predicted against actual inhibition efficiency, b) Inhibition efficiency against inhibitor conc. and temp., c) Inhibition efficiency against inhibitor conc. and time, d) Inhibition efficiency against temp. and time.

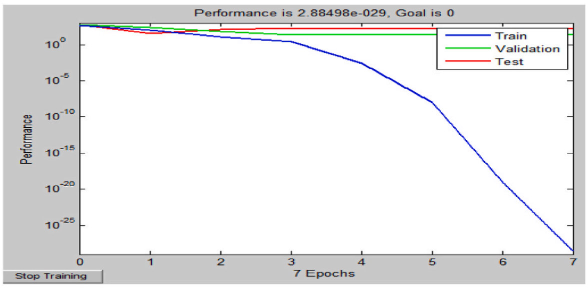

Fig. 4. Network performance evaluation for the efficiency of castor oil leaf as corrosion inhibitor of mild steel in H_2SO_4 media.

the response for given levels of each factor [15]. It is useful for identifying the relative impact of the factors by relating the factor coefficients.

3.2.2. Graphs of the RSM results

Graphical analyses of the results are displayed in Fig. 3; a) predicted against actual inhibition efficiency, b) inhibition efficiency against inhibitor concentration and temperature, c) inhibition efficiency against inhibitor concentration and time, and d) inhibition efficiency against temperature and time. The plot of predicted versus actual inhibitor's efficiency (IE) showed a linear graph; where the points clustered along the line of best fit. Thus, the obtained model adequately predicts the efficiency of the corrosion control process. All the 3-D plots showcase parabolic curves, which corroborates with the established quadratic model. Prior to the optimum point, IE

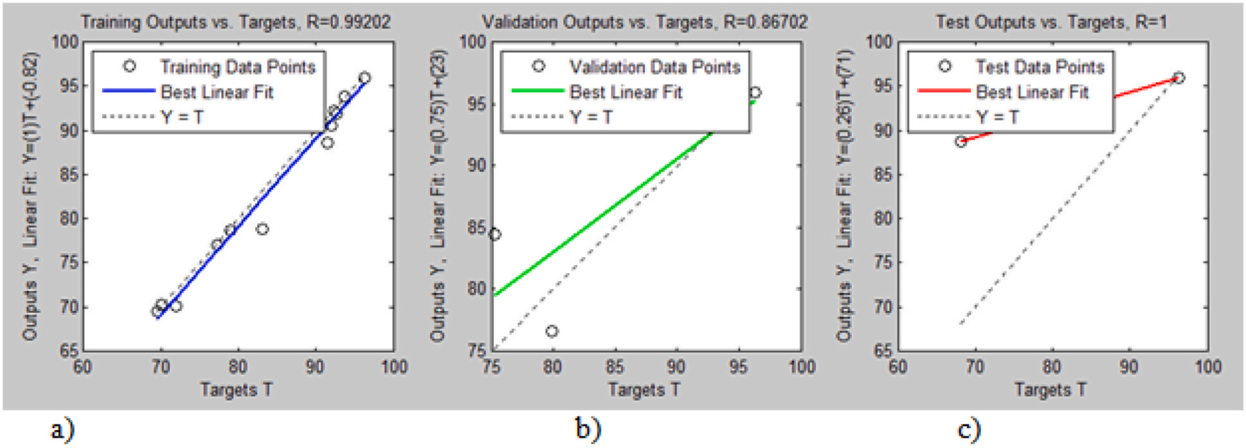

Fig. 5. Regression analysis of the network for the efficiency of castor oil leaf as corrosion inhibitor of mild steel in H_2SO_4 media: a) Training outputs versus targets, b) Validation outputs versus targets, c) Test outputs versus targets.

Table 4
Comparison of the RSM and ANN results.

Std	Run	A: Inh. conc., g/L	B: Temp. K	C: Time hr	Actual IE, %	RSM predicted IE, %	ANN predicted IE%
5	1	0.2	303	24	77.24	76.64	76.42
3	2	0.2	333	8	68.15	67.66	67.33
14	3	0.6	318	24	92.62	95.54	91.80
13	4	0.6	318	8	92.29	91.10	91.47
2	5	1.0	303	8	83.12	84.17	82.30
10	6	1.0	318	16	91.43	91.07	90.61
16	7	0.6	318	16	96.25	95.67	95.43
9	8	0.2	318	16	79.01	81.11	78.19
12	9	0.6	333	16	79.89	82.60	79.07
4	10	1.0	333	8	71.92	72.09	71.10
18	11	0.6	318	16	96.25	95.67	95.43
15	12	0.6	318	16	96.25	95.67	95.43
1	13	0.2	303	8	69.54	70.01	68.72
20	14	0.6	318	16	96.25	95.67	95.43
19	15	0.6	318	16	96.25	95.67	95.43
7	16	0.2	333	24	70.06	68.58	69.24
8	17	1.0	333	24	75.25	74.34	74.43
11	18	0.6	303	16	93.65	92.67	92.83
6	19	1.0	303	24	92.07	92.13	91.25
17	20	0.6	318	16	96.25	95.67	95.43

rose with rise in time and inhibitor's concentration. This is due to increase in the adsorption of the bio-molecules. The efficiency reduces with rise in temperature. This is because rise in temperature facilitates desorption of physically adsorbed molecules. It can also be credited to the rise in the solubility of the protective films. These findings are in agreement with previous research reports [22,23,31].

3.3. Artifitial neural network (ANN) analysis

Performance analysis of ANN for the modeling of the efficiency of castor oil leaf is presented in Fig. 4. The performance plot for the trained network displayed 7 epochs, suggesting that ANN is suitable for predicting the optimum efficiency of the castor oil leaf. The regressional plot graph is shown in Fig. 5 (a, b, c), were; a) training outputs versus targets, b) validation outputs versus targets, and c) test outputs versus targets were displayed. They revealed straight line graphs, which suggest that the ANN can effectively predict the experimental data.

3.4. Comparison of the results of the modeling tools

Table 4 presents the comparison of the RSM and ANN results. It showed the actual experimental results of the 20-run experimental design alongside the predicted values of the inhibition efficiencies. 96.25 % was obtained as the actual inhibition efficiency of castor oil leaf. This high level of inhibition efficiency may be attributed to the presence of long chain bio-molecular structures of the inhibitor

Table 5
Statistical comparison of the RSM and ANN predictions of the inhibition efficiency.

Parameters	RSM	ANN
RMSE	1.220236	0.820000
R^2	0.981709	0.991740
SEP	1.424062	0.956971

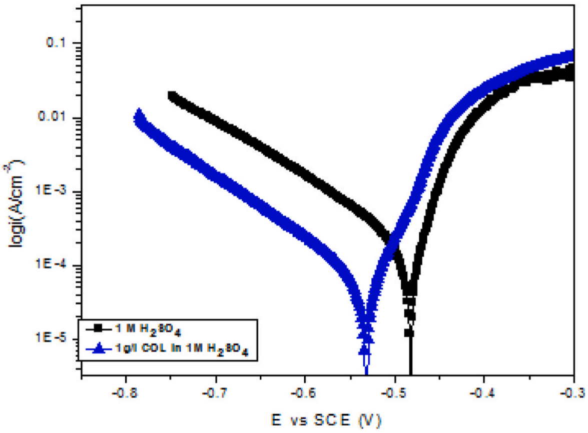

Fig. 6. Potentiodynamic polarization curves for mild steel in 1 M H_2SO_4 in the absence and presence of castor oil leaf extract at 30 °C.

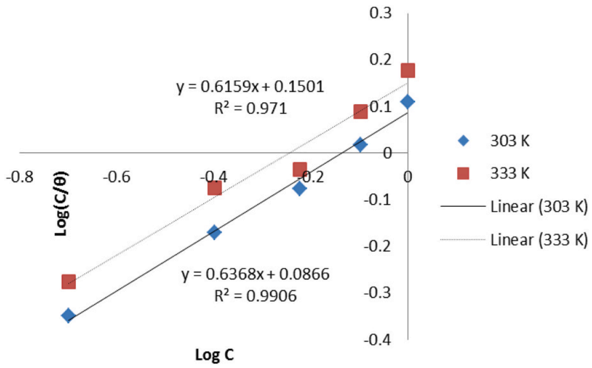

Fig. 7. Langmuir plot.

[32]. A comparative study between ANN and RSM was carried out so as to reveal the respective predictive performance and estimation capabilities by means of various statistical indicators. Results of the statistical analyses, which compared the capability of the modeling tools, are shown in Table 5. The correlation coefficient, R^2 indicates the goodness of fit for the model [29,33]. ANN gave high values of the determination coefficient (R^2) of 0.99174, compared to that of RSM, 0.981709. Also, ANN gave better prediction than RSM because the values of the RMSE and SEP were lower than those of RSM.

3.5. Results of the potentiodynamic polarization (PDP) techniques

The PDP results of the corrosion in the absence and presence of castor oil leaf are shown in Fig. 6. Considering the uninhibited and inhibited H_2SO_4 media, the curves shifted in both cathodic and anodic sides, which revealed that it is mixed-type inhibitor. It corroborates with the reports of Paul et al. [17] and Onukwuli and Omotioma [12]. It revealed specific effects of the inhibitor on the anodic and cathodic corrosion reactions [12,14,34]. The mechanisms of the cathodic and anodic partial reactions control the overall rate of corrosion. The molecules of the inhibitor become effective by attaching on the metal. As mixed-type inhibitor, leaf of castor oil is suitable for anodic and cathodic corrosion control [22,23,27].

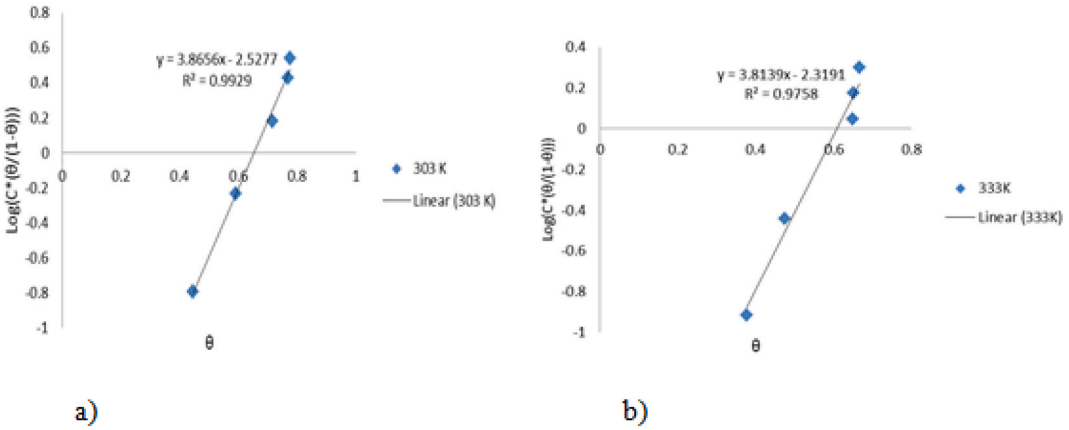

Fig. 8. Frumkin plot a) Adsorption at temperature of 303K, b) Adsorption at temperature of 333K.

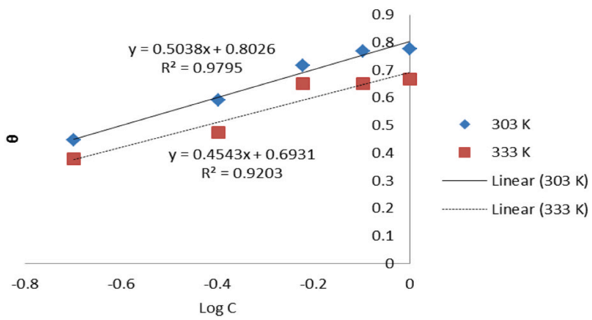

Fig. 9. Temkin plot.

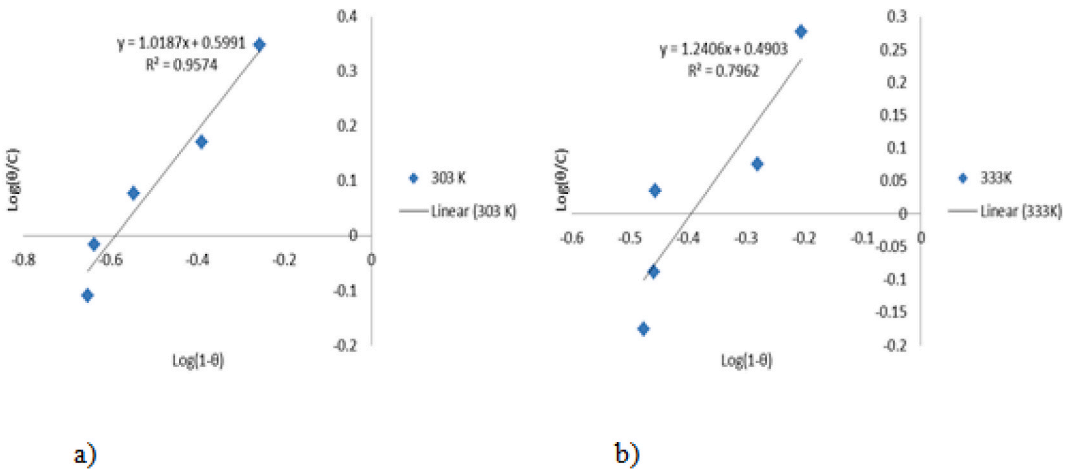

Fig. 10. Flory-Huggins plot.

3.6. Adsorption properties of the control process

In testing the mechanism of the inhibitor adsorption, the experimental data were fitted into physical adsorption isotherms of Langmuir, Frumkin, Temkin and Flory-Huggins; expressed in Figs. 7 and 8 (a, b), 9 and 10 (a, b) respectively. They all displayed linear graphs with corresponding linear Equations, from where values of the adsorption properties were obtained, shown in Table 6. Frumkin isotherm is best fitted isotherm because the coefficient of determination (R^2) values (0.9929 and 0.9758 at 303 K and 333 K respectively) are the closest to 1 (one) compared to those of other isotherms. The order of fitness is Frumkin > Langmuir > Temkin >

Table 6
Adsorption properties.

Isotherm	T (K)	R^2	K	ΔG_{ads} (kJ/mol)	α	a	x
Langmuir	303.0	0.9906	0.8192	−9.6	–	–	–
	333.0	0.9710	0.7078	−10.6	–	–	–
Frumkin	303.0	0.9929	0.0799	−3.8	1.9328	–	–
	333.0	0.9758	0.0984	−4.7	1.9070	–	–
Temkin	303.0	0.9790	39.30	−19.3	–	−2.289	–
	333.0	0.9200	33.61	−20.8	–	−2.536	–
Flory-Huggins	303.0	0.9570	3.9719	−13.6	–	–	1.018
	333.0	0.7960	3.0903	−14.2	–	–	1.240

Flory-Huggins**.** Positive values of the lateral interactive term α (1.9328 and 1.9070 at 303K and 333K respectively) showed that there was appreciable attraction between the bio-molecules of the castor oil leaf and the mild steel surface. Negative values of the attractive parameter (a) −2.289 and −2.536, signify that there was no chemical reaction at the mild steel-inhibitor interface. Recorded Gibb's free energy is lower than −40 kJ/mol. It confirms that the adsorption of the biomolecules is a physical adsorption mechanism (not chemisorption). This observation corroborates research reports of Onukwuli and Omotioma [12], and Azeez et al. [20] (see Fig. 9).

4. Conclusion

It was found that castor oil leaf contains methyl nicotinate and pyridine-4-carbohydrazide. The bio-molecular compounds contain heteroatoms of N, S and O, showcasing that the castor oil leaf has strong corrosion inhibitive properties. Bio-inspired control of the corrosion in H_2SO_4 was successfully achieved by heterocyclic molecules of the castor oil leaf. Comparatively, ANN gave better prediction of the efficiency of the castor oil leaf than RSM. Castor oil leaf should be applied as natural plant-based inhibitor for anodic and cathodic corrosion control processes. The result of this experiment would be a useful guide for academic and industrial researches.

CRediT authorship contribution statement

M. Omotioma: Writing – original draft, Software, Methodology, Data curation, Conceptualization. **O.D. Onukwuli:** Writing – review & editing, Supervision, Project administration, Formal analysis. **I.A. Nnanwube:** Writing – review & editing, Software, Project administration, Methodology, Formal analysis, Data curation.

Declaration of competing interest

The authors declare the following financial interests/personal relationships which may be considered as potential competing interests:Ikechukwu Nnanwube reports administrative support was provided by Madonna University Nigeria. Ikechukwu Nnanwube reports a relationship with Madonna University Nigeria that includes: employment. There are no additional relationships to declare. If there are other authors, they declare that they have no known competing financial interests or personal relationships that could have appeared to influence the work reported in this paper.

References

[1] L.W. El Khatib, H.T. Rahal, A.M. Abdel-Gaber, Synergistic effect between Fragaria ananassa and Cucurbita pepo L leaf extracts on mild steel corrosion in hydrochloric acid solutions, Protect. Met. Phys. Chem. Surface 56 (5) (2020) 1096–1106.
[2] R.S. Al-Moghrabi, A.M. Abdel-Gaber, H.T. Rahal, Corrosion inhibition of mild steel in hydrochloric and nitric acid solutions using willow leaf extract, Protect. Met. Phys. Chem. Surface 55 (2019) 603–607.
[3] M.Y. El Sayed, A.M. Abdel-Gaber, H.T. Rahal, Safranin—a potential corrosion inhibitor for mild steel in acidic media: a combined experimental and theoretical approach, J. Fail. Anal. Prev. 19 (4) (2019) 1174–1180.
[4] M. Kilo, H.T. Rahal, M.H. El-Dakdouki, A.M. Abdel-Gaber, Study of the corrosion and inhibition mechanism for carbon steel and zinc alloys by an eco-friendly inhibitor in acidic solution, Chem. Eng. Commun. 208 (12) (2021) 1676–1685.
[5] M.K. Pavithra, T.V. Venkatesha, M.K. Punith Kumar, H.C. Tondan, Inhibition of mild steel corrosion by Rabeprazole Sulfide, Corrosion Sci. 60 (2012) 104–111.
[6] G.S. Sajadi, R. Naghizade, L. Zeidabadinejad, Z. Golshani, M. Amiri, S.M.A. Hosseini, Experimental and theoretical investigation of mild steel corrosion control in acidic solution by Ranunculus arvensis and Glycine max extracts as novel green inhibitors, Heliyon 8 (10) (2022) e10983.
[7] A. Singh, A. Gupta, A.K. Rawat, K.R. Ansari, M.A. Quraishi, E.E. Ebenso, Cimetidine as an effective corrosion inhibitor for mild steel in hydrochloric acid, Int. J. Electrochem. Sci. 9 (12) (2014) 7614–7628.
[8] A. Popova, M. Christov, A. Vasilev, Mono-and Dicatonic Benzothiazolic Quaternary Ammonium Bromides as mild steel inhibitors, part III: influence of the temperature on the inhibitor process, Corrosion Sci. 94 (2015) 70–78.
[9] P. Satyabama, S. Rajendran, T.A. Nguyen, Corrosion inhibition of aluminium by oxalate self-assembling monolayer, Anti-corrosion Methods & Mater. 66 (6) (2019) 768–773.
[10] M. Omotioma, O.D. Onukwuli, I. Obiora-Okafo, Phytochemicals and inhibitive properties of Cashew extract as corrosion inhibitor of aluminium in H_2SO_4 medium, Lat. Am. Appl. Res. 49 (2019) 99–103.
[11] Y. Yang, W. Wu, X. Cheng, J. Zhao, B. Zhaol, X. Li, Corrosion mechanism of a new-type low-alloy corrosion resistant steel containing Sb used in acid environment, Anti-corrosion Methods & Mater. 68 (2) (2021) 85–94.
[12] O.D. Onukwuli, M. Omotioma, Optimization of the inhibition efficiency of mango extract as corrosion inhibitor of mild steel in 1.0M H_2SO_4 using response surface methodology, Journal of Chemical Technology and Metallurgy 51 (3) (2016) 302–314.
[13] M.E. Mashuga, L.O. Olasunkami, E.E. Ebenso, Experimental and theoretical investigation of the inhibitory effect of new pyradazine derivatives for the corrosion of mild steel in 1M HCL, J. Mol. Struct. 1136 (2017) 127–139.

[14] V.V. Torres, R.S. Amado, F. Camila, T.L. Fernadez, A.S.R. Carlos, A.G. Torres, D. Elian, Inhibitory action of aqueous coffee ground extracts on the corrosion of carbon steel in HCl solution, Corrosion Sci. 53 (2011) 2385–2392.

[15] M. Omotioma, O.D. Onukwuli, Modeling the corrosion inhibition of mild steel in HCl medium with the inhibitor of Pawpaw leaves extract, Port. Electrochim. Acta 34 (4) (2016) 287–294.

[16] C. Verma, M.A. Quarishi, E.E. Ebenso, I.B. Obot, A. El Assyry, 3-Amino Alkylated Indoles as corrosion inhibitors for mild steel in 1M HCL: experimental and theoretical Studies, J. Mol. Liq. 219 (2016) 647–660.

[17] P.K. Paul, M. Yadav, I.B. Obot, Investigation on corrosion protection behaviour and adsorption of carbonhydrazide-pyrazole compounds on mlild steel in 15% HCl solution: electrochemical and computational approach, J. Mol. Liq. 314 (2020) 11313.

[18] M.A. Qurishi, D.S. Chauhan, V.S. Saji, Heterocyclic biomolecules as green corrosion inhibitors, J. Mol. Liq. 341 (2021) 117265.

[19] H.T. Rahal, A.M. Abdel-Gaber, G.O. Younes, Inhibition of steel corrosion in nitric acid by sulfur containing compounds, Chem. Eng. Commun. 203 (4) (2016) 435–445.

[20] F.A. Azeez, O.A. Al-Rashed, A.A. Nazeer, Controlling of mild steel corrosion in acidic solution using environmentally friendly ionic liquid inhibitors: effect of alkyl chain, J. Mol. Liq. 265 (2018) 654–663, https://doi.org/10.1016/j.molliq.2018.05.093.

[21] O.D. Onukwuli, M. Omotioma, Study of bitter leaves extract as inhibitive agent in HCl medium for the treatment of mild steel through pickling, Portuagaliae Electrochemical Acta 37 (2) (2019) 115–121.

[22] O.D. Onukwuli, M. Omotioma, I. Obiora-Okafo, Thermometric and gravimetric analyses of aluminium corrosion control in HCl medium using *Ricinus Communis* extract, Port. Electrochim. Acta 38 (1) (2020) 19–28.

[23] V.C. Anadebe, O.D. Onukwuli, M. Omotioma, N.A. Okafor, Optimization and electrochemical study on the control of mild steel corrosion in hydrochloric acid solution with bitter kola leaf extract as inhibitor, S. Afr. J. Chem. 71 (2018) 51–61.

[24] H.S. Lozano-Puentes, J.J. Sánchez-Matiz, E. Ruiz-Sanchez, G.M. Costa, L.A. Díaz-Ariza, Guadua angustifolia Kunth leaves as a source for bioactive phenolic compounds: optimization of ultrasound-assisted extraction using response surface methodology and antioxidant activities, Heliyon 9 (12) (2023) e22445.

[25] M.S. Al-Otaibi, A.M. Al-Mayouf, M. Khan, A.A. Mousa, S.A. Al-Mazroa, H.Z. Alkhathlan, Corrosion inhibitory action of some plant extracts on the corrosion of mild steel in acidic media, Arab. J. Chem. 7 (2014) 340–346.

[26] X. Li, S. Deng, Inhibition effect of Dendrocalamus brandissi leaves extracts on aluminium in HCl, H_3PO_4 solutions, Corrosion Sci. 65 (2012) 299–308.

[27] V.C. Anadebe, O.D. Onukwuli, M. Omotioma, N.A. Okafor, Experimental theoretical modeling and optimization of inhibition efficiency of pigeon pea leaf extract as anti-corrosion agent of mild steel in acid environment, Mater. Chem. Phys. 233 (2019) 120–132.

[28] J. Xi, Y. Xue, Y. Xu, Y. Shen, Artificial neural network modeling and optimization of ultrahigh pressure extraction of green tea polyphenols, Food Chem. 141 (2013) 320–326.

[29] I.A. Nnanwube, D.O. Onukwuli, Modeling and optimization of galena dissolution in a binary solution of nitric acid and ferric chloride using artificial neural network coupled with genetic algorithm and response surface methodology, South Afr. J. Chem. Eng. 32 (2020) 68–77.

[30] J. Pilkington, C. Preston, R.L. Gomes, Comparison of response surface methodology (RSM) and artificial neural network (ANN) towards efficient extraction of Artemisinin from Artemisia Annua, Ind. Crop. Prod. 58 (2014) 15–24.

[31] O.O. Onukwuli, B.C. Udeh, M. Omotioma, I.A. Nnanwube, Corrosion inhibition of aluminium in hydrochloric acid medium using Cimetidine Drug as inhibitor: empirical and optimization Studies, Anti-Corrosion Method and Materials 68 (5) (2021) 385–395.

[32] C. Verma, M.A. Quarishi, K.Y. Rhee, Hydrophilicity and hydrophobicity consideration of organic surfactant compounds: effect of alkyl chain length on corrosion protection, Adv. Colloid Interface Sci. 306 (2022).

[33] O.D. Onukwuli, E. Chizoo, U.O. Akuzuo, R. Eyisi, Comparative Analysis of the Application of Artificial Neural Network-Genetic Algorithm and Response Surface Methods- Desirability Function for Predicting the Optimal Conditions for Biodiesel Synthesis from Chrysophyllum Albidum Seed Oil, vol. 125, Journal of Taiwan Institute of Chemical Engineers, 2021, pp. 153–167.

[34] B. Ramezanzadeh, M. Mehdipour, S.Y. Arman, M. Ramenzanzadeh, An electrochemical investigation of azole derivative on aluminum in 0.25M HCL solution using EN and EIS techniques, Anti-corrosion Methods & Mater. 64 (1) (2017) 10–22.